Malaya Journal of Matematik, Vol. 9, No. 1, 870-877, 2021

https://doi.org/10.26637/MJM0901/0153

Effect of couple stress on concentration of aerosols in an inclined channel with an applied electric and magnetic field

P. Meenapriya[1], K. Uma Maheswari[2]* and Nirmala P. Ratchagar[3]

Abstract

Aerosol particles are responsible for some serious respiratory and cardiovascular diseases. The main motive of the paper is to observe the effects of smog and haze through concentration of aerosols with and without chemical reaction, in order to improve atmospheric visibility. A mathematical model is developed which includes inclined channel containing couple stress fluid bounded by porous layers together with the effect of applied electric and magnetic field. The derived partial differential equations are solved using perturbation technique and the obtained solutions are displayed through graphs. Significant results have attained and there is a noticeable variation in results which is valid for the conclusion of study.

Keywords

Navier-stokes equation, Analytic approximation of solutions, Chemically reacting flows, Boundary value problems for linear higher-order PDEs, Electromagnetic fields.

AMS Subject Classification

76D05, 76M45, 80A32, 35G15, 83C50.

[1,2,3] *Department of Mathematics, Annamalai University, Chidambaram 608002, Tamil Nadu, India.*

***Corresponding author**: [2] umamohansusd@gmail.com

Article History: Received **24** January **2021**; Accepted **09** March **2021**

Contents

1 **Introduction** 870

2 **Mathematical Formulation** 871

3 **Method of Solution** 873

3.1 Concentration of smog (C_1)(when $\beta \neq 0$ and $i = 1$) . 874

3.2 Concentration of haze (C_2)(when $\beta = 0$ and $i = 2$) 874

4 **Results and Discussion** 874

4.1 Velocity graph 874

4.2 Concentration graph 874

5 **Conclusion** 876

References 876

1. Introduction

Mathematical models are effective tools that examine environmental and ecological impacts of pollution control and resource conservation. Ambient air pollution destroys over five million people every year globally. Air quality models are used to examine the air pollutants in the atmospheric layer closest to the ground which reduces visibility. Therefore, in order to limit visibility there is a need to study the concentration of aerosols in the fluid flow with and without chemical reaction.

Literatures on air pollutant concentration related to environmental issues are enormous. Larsen[9] presented a new mathematical model to relate air pollutant concentration to air quality standards and emission standards. Zeidan[13] illustrated the vital role played by mathematical models in examining the environmental issues.

When aerosols are congested by poor weather situations, tiny grains of dust particles accumulate and concentrate to form a low-hanging shroud called haze and aerosols react with smoke (chemical) to form smog. Both smog and haze suspended in the air lead to the deterioration of horizontal visibility and have a huge impact on human health. Cermak[5] presented a technique for automated detection of fog and low stratus distribution along the South- Western African coast. Mao et al[11] developed a 2D space model suitable for distinguishing different types of aerosols and its strong applicability. Meenapriya[12] developed a model to investigate the effects of aerosol dispersion in couple stress fluid.

Several studies have been reported on couple stress fluid under different physical situations. Owing to the importance of couple stress flow, Abdullahi et al[1] investigates the influence of MHD on a peristaltic flow of Newtonian fluid with couple stress through porous medium. The magneto hydrodynamic three dimensional flow of couple stress nano fluid thermophoresis and its Brownian motion was investigated by Hayat[7] through homotopy analysis technique. Khan et al[8] found the exact solution of two dimensional MHD couple stress and heat transfer is also analysed using travelling wave phenomenon.

Literatures on fluid flow in an inclined channel are enormous. Aina and Malgwi[3] investigates the laminar flow of a viscous, incompressible, electrically conducting fluid in an inclined micro porous channel with transversely applied magnetic field. Ahmed et al[2] studied analytically the oscillatory hydromagnetic flow of a viscous, incompressible, electrically conducting, non-Newtonian fluid in an inclined rotating channel with nonconducting walls incorporating couple stress effects. The effect of wall porosity on the two-dimensional steady-state incompressible laminar flow of a fluid in a channel having rectangular cross section has been investigated by Berman[4]. Cheng[6] used Prandtl coordinate transformation and cubic spline method to study the natural convection heat transfer from an inclined wavy plate in a bidisperse porous medium. Leblond[10] gave a powerful reductive perturbation technique to solve nonlinear equations in an effective way and some applications pertaining to it.

The above studies motivated to examine the couple stress effects of smog and haze in the inclined channel through aerosol concentration both in the presence and absence of chemical reaction using perturbation technique. Numerical calculations are being computed and results are portrayed graphically.

2. Mathematical Formulation

Consider two dimensional flow of an incompressible couple stress fluid, which is assumed to be poorly conducting. The rectangular coordinate system (x,y) is sketched in Figure 1, which is expressed to model the flow with the channel is symmetric about x-axis and inclined at an angle with the horizontal bounded by porous layers on both sides.The electric field is applied through electrodes with electric potentials $\phi = (\frac{V}{h})x$ at $y=-h$, $\phi = \frac{V}{h}(x-x_0)$ at $y=h$. The uniform magnetic field is applied in y-direction, neglecting the induced electric and magnetic field. The governing equations are solved using the perturbation technique and let homogeneous first-order chemical reaction (K) takes place inside the channel with D as the mass diffusivity. The fluid is assumed to be driven by laminar flow with constant pressure gradient.

Based on all the assumptions made above the principal equations for the fluid flow can be written as,

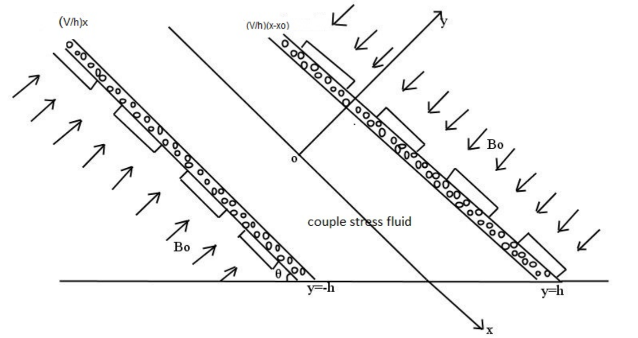

Figure 1. Physical configuration

Continuity equation

$$\frac{\partial u}{\partial x}+\frac{\partial v}{\partial y}=0 \tag{2.1}$$

x- component of momentum equation

$$\rho[\frac{\partial u}{\partial t}+u\frac{\partial u}{\partial x}+v\frac{\partial u}{\partial y}]=-\frac{\partial p}{\partial x}+\rho g sin(\theta)+ \mu(\frac{\partial^2 u}{\partial x^2}+\frac{\partial^2 u}{\partial y^2})-\lambda[\frac{\partial^4 u}{\partial x^4}+\frac{\partial^4 u}{\partial y^4}+2\frac{\partial^2 u}{\partial x^2}\frac{\partial^2 u}{\partial y^2}]+ \rho_e E_x-\sigma_c u B_0^2 \tag{2.2}$$

y- component of momentum equation

$$\rho[\frac{\partial v}{\partial t}+u\frac{\partial v}{\partial x}+v\frac{\partial v}{\partial y}]=-\rho g cos(\theta)+\mu\frac{\partial^2 v}{\partial x^2}+\frac{\partial^2 v}{\partial y^2}- \lambda[\frac{\partial^4 v}{\partial x^4}+\frac{\partial^4 v}{\partial y^4}+2\frac{\partial^2 v}{\partial x^2}\frac{\partial^2 v}{\partial y^2}] \tag{2.3}$$

Species equation

$$\frac{\partial C_i}{\partial t}+u\frac{\partial C_i}{\partial x}+v\frac{\partial C_i}{\partial y}=D(\frac{\partial^2 C_i}{\partial x^2}+\frac{\partial^2 C_i}{\partial y^2})-KC_i \tag{2.4}$$

where p is the pressure of the fluid, E_x is the electric field, ρ is the density of the fluid, and μ is the co-efficient of viscosity. The applied magnetic field B_0 is functional in y-axis and ρ is the density of charge distribution. The concentration of aerosols is represented by C_i also we assume $\beta \neq 0$ when i=1, and $\beta = 0$ when i=2. To solve the governing equations Beaver Joseph slip conditions and vanishing of couple stress boundary conditions are used to sculpt the boundary effects for velocity.

$$u=0, \frac{\partial^2 u}{\partial y^2}=0, \ \ at \ \ y=\pm h \tag{2.5}$$

$$v=0, \frac{\partial^2 v}{\partial y^2}=0, \ \ at \ \ y=\pm h \tag{2.6}$$

$$\frac{\partial u}{\partial y}=\frac{-\alpha_p}{\sqrt{k}}(u-u_p), \frac{\partial v}{\partial y}=0, \quad C_i=C_0(1+\varepsilon e^{\mathbf{i}(\alpha x+wt)}), \ \ at \ \ y=h \tag{2.7}$$

$$\frac{\partial u}{\partial y} = \frac{\alpha_p}{\sqrt{k}}(u-u_p), C_i = C_0, \ \ at \ \ y=-h \quad (2.8)$$

$$\frac{\partial v}{\partial y} = 0, \frac{\partial C_i}{\partial y} = C_0 \varepsilon e^{\mathbf{i}(\alpha x + wt)}, \ \ at \ \ y=0 \quad (2.9)$$

Where u_p is the Darcy velocity of the porous layer and $u_p = \frac{-k}{\mu}(\frac{\partial p}{\partial x})$ represents Darcy law, α_p is the slip parameter, k is the permeability of the porous layer, α is the streamwise wave number, w is the frequency parameter, ε is the perturbation parameter, $\mathbf{i}$ is the imaginary number. To make (2.1) to (2.9) dimensionless the following dimensionless quantities are introduced,
$x^* = \frac{x}{h}; y^* = \frac{y}{h}; u^* = \frac{u}{u_0}; v^* = \frac{v}{v_0}; p^* = \frac{p}{\rho u_0{}^2}; t^* = \frac{t}{t_0};$
$u_p^* = \frac{u_p}{u_0}; \rho_e^* = \frac{\rho_e}{(\frac{\varepsilon_0 V}{h^2})}; E_x^* = \frac{E_x}{(\frac{V}{h})}; \beta^2 = \frac{h^2 k}{D}; l^2 = \frac{\lambda}{\mu}; C_i{}^* = \frac{C_i}{C_0};$
The chemical reaction rate parameter is β, λ is the rotational viscosity, l is the dimension of length and V is the applied constant electric potential due to embedded electrodes at the boundaries. The porous parameter σ is given by $\sigma = \frac{h}{\sqrt{k}}$, the couple stress parameter $a = \frac{h}{l}$, gravity parameter $G = \frac{\rho g h}{\mu u_0}$, the electric number $W_e = \frac{\varepsilon_0 V^2}{h \mu u_0}$, the Hartmann number $M^2 = \frac{\sigma_c B_0^2 h^2}{\mu}$. After non dimensionalising the above governing equations and boundary conditions neglecting asterisk we obtain,

$$\frac{\partial u}{\partial x} + \frac{\partial v}{\partial y} = 0 \quad (2.10)$$

$$\left(\frac{\partial^4 u}{\partial x^4} + \frac{\partial^4 u}{\partial y^4}\right) + 2u_0 \frac{\partial^2 u}{\partial x^2}\frac{\partial^2 u}{\partial y^2} - a^2\left(\frac{\partial^2 u}{\partial x^2} + \frac{\partial^2 u}{\partial y^2}\right) + \frac{Rea^2}{2}\left(\frac{2u_0}{t_0}\frac{\partial u}{\partial t} + u\frac{\partial u}{\partial x} + v\frac{\partial u}{\partial y}\right) + a^2 Re \frac{\partial p}{\partial x} - a^2 hGsin[\theta] - a^2 We \rho_e E_x + a^2 M^2 u = 0 \quad (2.11)$$

$$\frac{\partial^4 v}{\partial x^4} + \frac{\partial^4 v}{\partial y^4} + 2\frac{\partial^2 v}{\partial x^2}\frac{\partial^2 v}{\partial y^2} - a^2 \frac{\partial^2 v}{\partial x^2} + \frac{\partial^2 v}{\partial y^2} + a^2 Re\left(\frac{u_0}{t_0}\right)\frac{\partial v}{\partial t} + a^2 Re\left(u\frac{\partial v}{\partial x} + v\frac{\partial v}{\partial y}\right) + a^2 hGcos[\theta] = 0 \quad (2.12)$$

$$\frac{\partial^2 C_i}{\partial x^2} + \frac{\partial^2 C_i}{\partial y^2} - \frac{u_0 h}{D}\left(u\frac{\partial C_i}{\partial x} + v\frac{\partial C_i}{\partial y}\right) - \frac{h^2}{Dt_0}\left(\frac{\partial C_i}{\partial t}\right) - \beta^2 C_i = 0 \quad (2.13)$$

and the boundary conditions are

$$u = 0, \frac{\partial^2 u}{\partial y^2} = 0, \ \ at \ \ y = \pm 1 \quad (2.14)$$

$$v = 0, \frac{\partial^2 v}{\partial y^2} = 0, \ \ at \ \ y = \pm 1 \quad (2.15)$$

$$\frac{\partial u}{\partial y} = \frac{-\alpha_p}{\sqrt{k}}(u-u_p), \frac{\partial v}{\partial y} = 0, \quad C_i = 1 + \varepsilon e^{\mathbf{i}(\alpha x + wt)}, \ \ at \ \ y = 1 \quad (2.16)$$

$$\frac{\partial u}{\partial y} = \frac{\alpha_p}{\sqrt{k}}(u-u_p), C_i = 1, \ \ at \ \ y=-1 \quad (2.17)$$

$$\frac{\partial v}{\partial y} = 0, \frac{\partial C_i}{\partial y} = \varepsilon e^{\mathbf{i}(\alpha x + wt)}, \ \ at \ \ y=0 \quad (2.18)$$

To determine the velocity of the fluid, we need to evaluate the value of $\rho_e E_x$ in x- momentum equation. Using conservation of charges equation and Maxwell's equation, the value of $\rho_e E_x$ is calculated as given below.
Conservation of charges

$$\frac{\partial \rho_e}{\partial t} + \rho_e(\vec{q} \cdot \nabla) + \nabla \cdot \vec{J} = 0 \quad (2.19)$$

Maxwell's equation

$$\nabla \cdot \vec{E} = \frac{\rho_e}{\varepsilon_0}(Gausslaw) \quad (2.20)$$

$$\frac{-\partial B_0}{\partial t} = \nabla \times \vec{E}(Faraday'slaw) \quad (2.21)$$

$$\vec{J} = \sigma_c(\vec{E} + \vec{u} \times B_0)(Ohm'slaw) \quad (2.22)$$

In a poorly conducting couple stress fluid, the induced magnetic field is negligibly small compared to an electric field and hence the current density is $\vec{J} = \sigma_c(\vec{E})$and the electrical conductivity $\sigma_c \prec\prec 1$and hence any perturbation on it is negligible and so it depends upon the conduction temperature T_b. So (2.19) reduces to $\frac{\partial J}{\partial y} = 0$ and the equation of electric potential reduces to,

$$\frac{\partial^2 \phi}{\partial y^2} - \frac{1}{\sigma_c}\frac{\partial \phi}{\partial y}\frac{\partial \sigma_c}{\partial y} = 0 \quad (2.23)$$

with

$$\sigma_c = \sigma_0(1 + \alpha_h(T_b - T_0)) \quad (2.24)$$

where α_h is the volumetric expansion coefficient and T_b is the solution of equation $\frac{d^2 T_b}{dy^2}$ which is solved using dimensionless quantities, $(T_b)^* = \frac{T_b}{\Delta T}$; $\eta = \frac{y}{h}$; and the boundary conditions are $T_b = T_0$ at $\eta = -1$ and $T_b = T_1$ at $\eta = 1$. Hence we obtain the equation $T_b - T_0 = \frac{\Delta T(y+h)}{2h}$, where $\Delta T = T_1 - T_0$. Using this value in (2.24), we get $\sigma_c = \sigma_0(e^{\alpha_c(y+h)})$ and solving (2.23) using the boundary condition, $\phi = xPe$ at $y = -1$, and $\phi = (x - x_0)Pe$ at $y = 1$, we get the value of $\phi = (x - \frac{x_0 e^{\alpha_c h} - e^{\alpha_c y}}{2sinh(\alpha_c)})Pe$. Now consider $\rho_e E_x = (\nabla \cdot E)E_x$,

since$E_x = -1$ and $E = -\nabla\phi$ then $\rho_e E_x = (\nabla^2\phi(-1))$ hence $\rho_e E_x = \frac{\alpha_c^2 Pex_0 e^{-\alpha_c y}}{2sinh(\alpha_c h)} = a_1 e^{-\alpha_c y}$, where$a_1 = \frac{\alpha_c^2 Pex_0}{2sinh(\alpha_c h)}$.
After substituting $\rho_e E_x$, equation(2.11) becomes

$$(\frac{\partial^4 u}{\partial x^4}+\frac{\partial^4 u}{\partial y^4})+2u_0\frac{\partial^2 u}{\partial x^2}\frac{\partial^2 u}{\partial y^2}- a^2(\frac{\partial^2 u}{\partial x^2}+\frac{\partial^2 u}{\partial y^2})+(\frac{a^2 Re}{2})(\frac{2u_0\partial u}{t_0\partial t}+u\frac{\partial u}{\partial x}+v\frac{\partial u}{\partial y})+ a^2 Re\frac{\partial p}{\partial x}-a^2 hGsin(\theta)-a^2 Wea_1 e^{-\alpha_c y}+a^2M^2u=0 \tag{2.25}$$

3. Method of Solution

Perturbation technique is used to evaluate the values of velocity and concentration of air pollutants. Disintegrating the flow variables into steady base state quantities denoted by upper case and two-dimensional linear perturbed quantities denoted by $\widetilde{()}$ symbol as follows,

$u(x,y) = U_B(y)+\widetilde{u}(y)\varepsilon e^{\mathbf{i}(\alpha x+wt)}+o(\varepsilon^2)$
$v(x,y) = \widetilde{v}(y)\varepsilon e^{\mathbf{i}(\alpha x+wt)}+o(\varepsilon^2)$
$p(x,y) = P_B(x)+\widetilde{p}(y)\varepsilon e^{\mathbf{i}(\alpha x+wt)}+o(\varepsilon^2)$
$C_i(x,y) = C_{B_i}(y)+\widetilde{C}_i(y)\varepsilon e^{\mathbf{i}(\alpha x+wt)}+o(\varepsilon^2)$

After decomposing the above equation into base and perturbed parts, the solution of the base part are obtained analytically and that of the perturbed part are obtained numerically. Splitting (2.10), (2.12) to (2.18), (2.25) and neglecting the higher orders of perturbation parameter ε, the base part and perturbed part equations of velocities and concentration are obtained. Assuming the flow to be steady the following set of partial differential equations are derived.
Base part equations

$$\frac{\partial^4 U_B}{\partial y^4}-a^2(\frac{\partial^2 U_B}{\partial y^2})+a^2M^2U_B = a^2hGsin(\theta)-a^2Rea_2+Wea_1e^{\alpha_c y} \tag{3.1}$$

$$\frac{\partial^2 C_{B_i}}{\partial y^2}-\beta^2 C_{B_i}=0 \tag{3.2}$$

and the perturbed part equations are

$$\frac{\partial\widetilde{v}}{\partial y}=\widetilde{u}a_3 \tag{3.3}$$

$$\frac{\partial^4\widetilde{u}}{\partial y^4}-a^2\frac{\partial^2\widetilde{u}}{\partial y^2}+\widetilde{u}(\alpha^4+a^2\alpha^2-2u_0a^2\frac{\partial^2 U_B}{\partial y^2} -(\frac{a^2a_3Re}{2})U_B-(\frac{a^2a_4Reu_0}{t_0})+M^2a^2) -a_3a^2\widetilde{p}Re+\widetilde{v}\frac{a^2Re}{2}\frac{\partial U_B}{\partial y}=0 \tag{3.4}$$

$$\frac{\partial^4\widetilde{v}}{\partial y^4}-a^2\frac{\partial^2\widetilde{v}}{\partial y^2}+\widetilde{v}(\alpha^4+\alpha^2a^2-\frac{a^2a_4Reu_0}{t_0})=0 \tag{3.5}$$

$$\frac{\partial^2\widetilde{C}_i}{\partial y^2}+\widetilde{C}_i((\frac{u_0ha_3}{D})U_B-\alpha^2-\beta^2-a_4\frac{h^2}{Dt_0}) -\widetilde{v}\frac{\partial C_{B_i}}{\partial y}\frac{u_0h}{D}=0 \tag{3.6}$$

where $a_2=\frac{\partial p_B}{\partial x}$,$a_3=\alpha tan(\alpha x+wt)$,$a_4=wtan(\alpha x+wt)$ and the boundary conditions are, base part boundary conditions

$$U_B=0, \frac{\partial^2 U_B}{\partial y^2}=0, \ at \ \ y=\pm 1 \tag{3.7}$$

$$\frac{\partial U_B}{\partial y}=\frac{-\alpha_p}{\sqrt{k}}(U_B-u_p), C_{B_i}=1, \ at \ \ y=1 \tag{3.8}$$

$$\frac{\partial U_B}{\partial y}=\frac{\alpha_p}{\sqrt{k}}(U_B-u_p), C_{B_i}=1, \ at \ \ y=-1 \tag{3.9}$$

$$\frac{\partial C_{B_i}}{\partial y}=0, \ at \ \ y=0 \tag{3.10}$$

and the perturbed part boundary conditions are

$$\widetilde{u}=0, \frac{\partial^2\widetilde{u}}{\partial y^2}=0, \ at \ \ y=\pm 1 \tag{3.11}$$

$$\frac{\partial\widetilde{u}}{\partial y}=-\alpha\sigma\widetilde{u}, \widetilde{C}_i=0, \ at \ \ y=1 \tag{3.12}$$

$$\widetilde{v}=0, \frac{\partial^2\widetilde{v}}{\partial y^2}=0, \ at \ \ y=\pm 1 \tag{3.13}$$

$$\widetilde{v}=1, \frac{\partial\widetilde{C}_i}{\partial y}=1, \ at \ \ y=0 \tag{3.14}$$

The base part solution of velocity is derived from (3.1) and is given as,

$$U_B = Acosh(m_1y)+Bsinh(m_1y)+Ccosh(m_3y)+ Dsinh(m_3y)+b_1+b_2e^{-\alpha_c y} \tag{3.15}$$

The value of the constants A, B, C and D are calculated using boundary conditions (3.7), (3.8) and (3.9) are given in appendix. Next to substitute the values of U_B, $\frac{\partial^2 U_B}{\partial y^2}$ in equation (3.4) and (3.5) we get,

$$\frac{\partial^4\widetilde{u}}{\partial y^4}-a^2\frac{\partial^2\widetilde{u}}{\partial y^2}-\widetilde{u}(b_3-b_4cosh(m_1y)-b_5sinh(m_3y)- b_6cosh(m_3y)-b_7sinh(m_3y)-b_8e^{-\alpha_c y})+\widetilde{v}(b_9sinh(m_1y)+ b_{10}cosh(m_1y)+b_{11}sinh(m_3y)+b_{12}cosh(m_3y)- b_{13}e^{-\alpha_c y})-b_{14}=0 \tag{3.16}$$

$$\frac{\partial^4\widetilde{v}}{\partial y^4}-a^2\frac{\partial^2\widetilde{v}}{\partial y^2}+\widetilde{v}(b_{15}-b_{16}cosh(m_1y)- b_{17}sinh(m_1y)-b_{18}cosh(m_3y)-b_{19}sinh(m_3y)- b_{20}e^{-\alpha_c y})=0 \tag{3.17}$$

Where $b_2, b_3, \ldots b_{14}, \ldots, b_{20}$ are constants obtained when simplification given in appendix. The above two perturbed equations (3.16) and (3.17) are solved for $\widetilde{u}, \widetilde{v}$ numerically using MATHEMATICA, and hence velocities are plotted as graphs. The concentration of air pollutants with and without chemical reaction are discussed in the following subsections.

3.1 Concentration of smog (C_1)(when $\beta \neq 0$ and $i = 1$)

The base part of C_1 is C_{B_1} and its solution is obtained from (3.2) is given by,

$$C_{B_1} = E cosh(\beta y) + F sinh(\beta y) \tag{3.18}$$

Using boundary conditions (3.8) to (3.10) we get $E = \frac{1}{cosh(\beta)}$, F=0. The perturbed part equation of C_1, after substituting the values of U_B, C_{B_1} is given as,

$$\frac{\partial^2 \widetilde{C_1}}{\partial y^2}(c_1 cosh(m_1 y) + c_2 sinh(m_1 y) + c_3 cosh(m_3 y) + c_4 sinh(m_3 y) + c_5 e^{-\alpha_c y}) + c_6 - \widetilde{v}(c_7 sinh(\beta y) + c_8 cosh(\beta y)) = 0 \tag{3.19}$$

This perturbed equations is solved numerically subject to the boundary conditions prescribed in (3.12) and (3.14) graphs are plotted for concentration of smog (C_1) using MATHEMATICA.

3.2 Concentration of haze (C_2)(when $\beta = 0$ and $i = 2$)

If no chemical reaction takes place in the channel then the reaction rate parameter is zero, the corresponding base part of C_2 is C_{B_2} and its equation is given from (3.2),

$$\frac{\partial^2 C_{B_2}}{\partial y^2} = 0 \tag{3.20}$$

The solution of C_{B_2} is got by integrating the above equation twice so,

$$C_{B_2} = Gy + H \tag{3.21}$$

The constants G,H are calculated using boundary conditions described in (3.12) and (3.14) which are given by G=0, H=1. The real perturbed equation of concentration without chemical reaction is,

$$\frac{\partial^2 \widetilde{C_2}}{\partial y^2} + C_2((\frac{u_0 h a_3}{D})U_B - \alpha^2 + \frac{h^2 a_4}{D t_0}) - \widetilde{v}\frac{\partial C_{B_i}}{\partial y}\frac{u_0 h}{D} = 0 \tag{3.22}$$

after substituting the values of U_B, C_{B_2} (3.22) can be rewritten as,

$$\frac{\partial^2 \widetilde{C_2}}{\partial y^2}(c_1 cosh(m_1 y) + c_2 sinh(m_1 y) + c_3 cosh(m_3 y) + c_4 sinh(m_3 y) + c_9) - \widetilde{v} c_{10} = 0 \tag{3.23}$$

Equation (3.23) is solved numerically for $\widetilde{C_2}$ and graphical solution is obtained for C_2 using MATHEMATICA. The value of constants c_1 to c_9 are given in appendix. The solution of the perturbed equations are obtained in an elegant way and the results are observed through graphs and are discussed briefly in the proceeding section.

4. Results and Discussion

4.1 Velocity graph

Graphs are sketched to see the effects of velocity and concentration distributions for different flow parameters. Figure 2 depicts velocity plots for different values of Hartmann number (M) and gravity parameter (G). It shows that an increase in Hartmann number velocity declines while increasing the gravity parameter velocity increases. Figure 3 elucidates the plots of velocity for few values of electric number (We) and couple stress parameter (a). It is apparent that velocity reduces when there is an increase in both electric number and couple stress parameter. Figure 4 illustrates the velocity plots for some values of angle of inclination (θ) with increasing channel inclination, velocity accelerates.

4.2 Concentration graph

The concentration of smog (C_1) is shown for few values of reaction rate parameter in figure 5. It conveys that by increasing the rate of the reaction, smog concentration descends. Both the concentration of smog (C_1) and the concentration of haze (C_2) are presented in the following figures for different parameters. Figure 6 shows plots of concentration for some values of Hartmann number. Smog concentration increases when Hartmann number increases, while haze concentration declines when increasing Hartmann number. Concentration profile for some values of electric parameter are displayed in figure 7. It is observed from the figure that smog concentration enhances and haze concentration reduces when there is an increase in electric number. Figure 8 illustrates the concentration plots for different values of gravity parameter. It clearly shows that increasing the gravity parameter, both smog concentration and haze concentration declines.Concentration profile for some values of couple stress parameter are presented in figure 9. It tells us that smog concentration declines when there is an increase in couple stress parameter. Also enhancing the couple stress effects haze concentration increases.

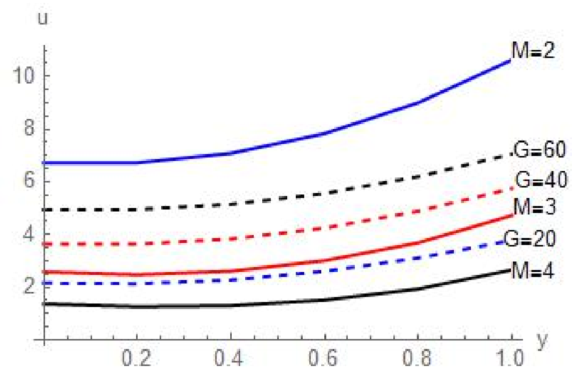

Figure 2. Plots of velocity for different values of Hartmann number and gravity parameter

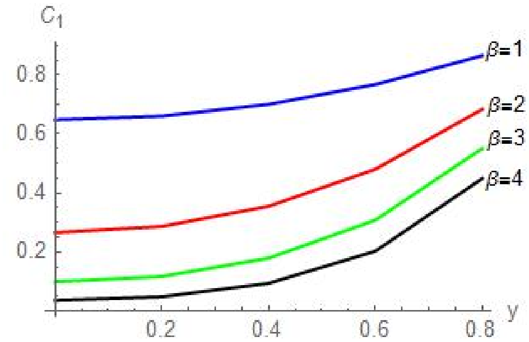

Figure 5. Concentration of smog for some values of reaction rate parameter

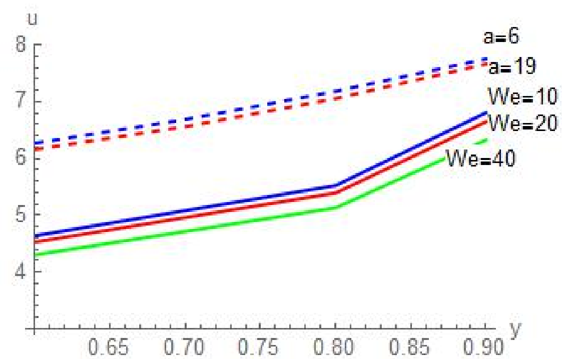

Figure 3. Velocity plots for some values of couple stress parameter and electric number

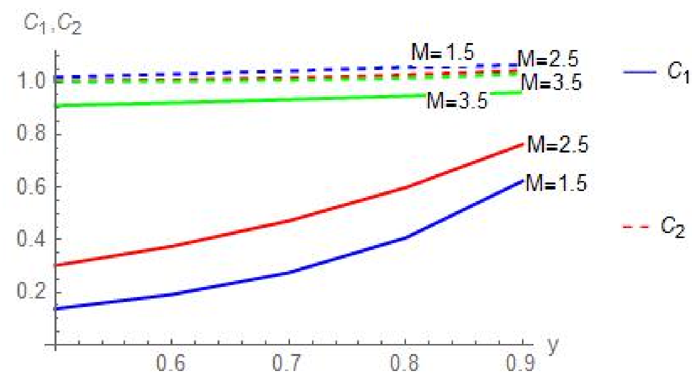

Figure 6. Concentration plots for some values of Hartmann number

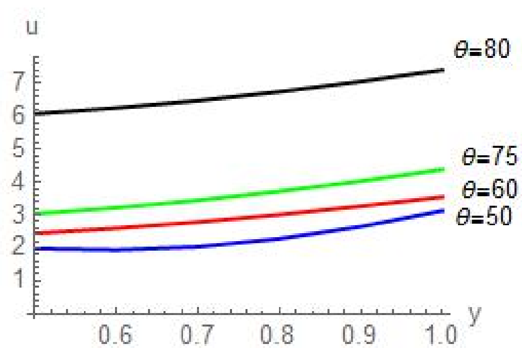

Figure 4. Velocity profile for some values of angle of inclination

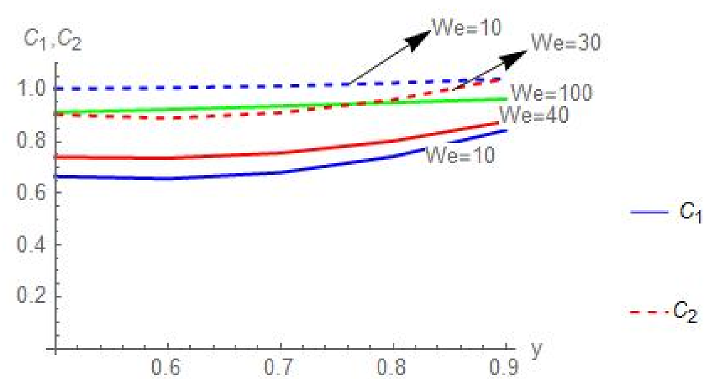

Figure 7. Concentration profile for different values of electric number

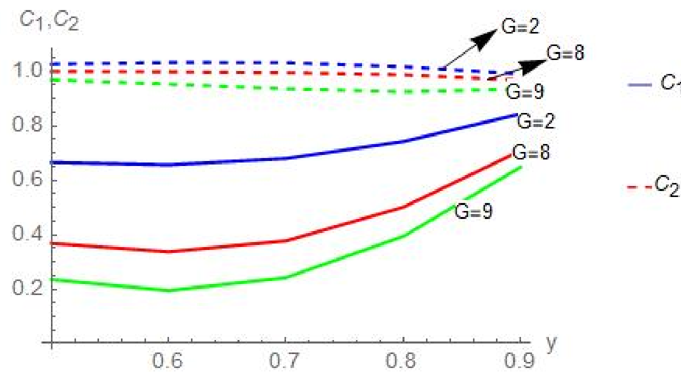

Figure 8. Concentration of smog and haze for various values of gravity parameter

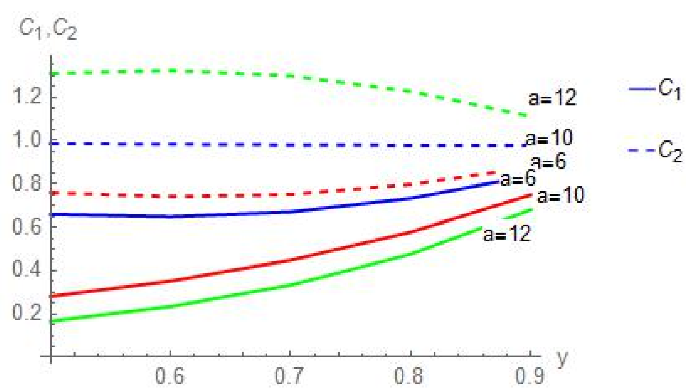

Figure 9. Concentration profile for different values of couple stress parameter

From the graphs it is clearly noted that there is no considerable reduction of smog concentration when there is an increase in both electric and magnetic field. Also graphs depicts that couple stress parameter has no effect in reducing haze concentration.

5. Conclusion

A two dimensional model with inclined channel of couple stress fluid bounded by porous layers with the applied electric and magnetic field is studied. From the study it is concluded that smog concentration is reduced by enhancing rate of the chemical reaction, inducing the couple stress effect and by raising gravity parameter. Also haze concentration is lowered by accelerating gravity parameter and by increasing the effect of electric and magnetic field. Hence concentration of aerosols are reduced in order to enhance atmospheric visibility.

References

[1] A. M. Abdulhadi and A. W. Saleh, Effects of couple stress and porous medium on transient magneto peristaltic flow under the action of heat transfer, *IOSR Journal of Mathematics* 12(2016), 71–83. https://doi.org/10.9790/5728-1204057183

[2] S. Ahmed and O.A. Be, A couple stress fluid modeling on free convection oscillatory hydromagnetic flow in an inclined rotating channel,*Engineering physics and mathematics* (2014), 1249–1265. https://doi.org/10.1016/j.asej.2014.04.006

[3] B.Aina and P.B. Malgwi, MHD Convection Fluid and Heat Transfer in an Inclined Micro-Porous-Channel,*Nonlinear Engineering* 8(2019), 755-763.

[4] A. S. Berman, Laminar flow in channels with porous walls, *Journal of Applied Physics.* 24 (1953), 1232-1235. https://doi.org/10.1063/1.1721476

[5] J. Cermak, Low clouds and fog along the South-Western African coast — Satellite-based retrieval and spatial patterns,*Atmospheric Research* 116(2012), 15—21. https://doi.org/10.1016/j.atmosres.2011.02.012

[6] C. Cheng, Natural convection heat transfer from an inclined wavy plate in a bidisperse porous medium, *International Communications in Heat and Mass Transfer* 43 (2013), 69—74. https://doi.org/10.1016/j.icheatmasstransfer.2013.01.001

[7] T. Hayat, A. Aziz, T. Muhammad, and B. Ahmad, Influence of Magnetic Field in Three- Dimensional Flow of Couple Stress Nanofluid over a Nonlinearly Stretching Surface with Convective Condition, *Plos one.* (2015), 1—18. https://doi.org/10.1371/journal.pone.0145332

[8] N. A. Khan, H. Khan and S. A. ali, Exact solutions for MHD flow of couple stress fluid with heat transfer, *Journal of the Egyptian Mathematical Society*, 24(2016), 125–129. https://doi.org/10.1016/j.joems.2014.10.003

[9] R. I. Larsen, A new mathematical model of air pollutant concentration averaging time and frequency, *Journal of the Air Pollution Control Association*, 19(1969), 24—30. https://doi.org/10.1080/00022470.1969.10466453

[10] H. Leblond, The reductive perturbation method and some of its applications, *Journal of Physics B: Atomic, Molecular and Optical Physics*, 41(2008). https://doi.org/10.1088/0953-4075/41/4/043001

[11] Q. Mao, C. Huang, Q. Chen, H. Zhang, and Y. Yuan, Satellite-based identification of aerosol particle species using a 2D-space aerosol classification model, *Atmospheric Environment*, 219(2019). https://doi.org/10.1016/j.atmosenv.2019.117057

[12] P. Meenapriya, Effect of couple stress and impact of chemical reaction on behaviour of atmospheric aerosols, *Advances in Mathematics: Scientific Journal.*, 9(2020), 2219–2232.

[13] B.A. Zeidan, Mathematical modeling of environmental problems, *Environmental Science and Engineering, Instrument, Modeling and Analysis*, 7(2017), 422—461.

Appendix

$A = \frac{(-b_{22}+b_{21}m_3^2)Sech[m_1]}{m_1^2-m_3^2}$; $B = -\frac{(b_{23}-b_{24})Cosh[m_3]}{m_1(Cosh[m_1]-Cosh[m_3])}$;

$C = -\frac{(b_{22}-b_{21}m_1^2)Sech[m_3]}{m_1^2-m_3^2}$; $D = -\frac{(b_{23}+b_{24}Cosh[m_1])}{m_3Cosh[m_1]-Cosh[m_3]}$;

$b_1 = \frac{(Ra_2-hGSin[\Theta])}{M^2}$; $b_2 = \frac{W_e a_1 a^2}{\alpha_c^2-a^2M^2}$;

$b_3 = \alpha^4 + a^2\alpha^2 - M^2a^2 - \frac{Ra^2a_3b_1}{2} - \frac{Ra^2a_4u_0}{t_0}$;

$b_4 = 2u_0\alpha^2Am_1^2 + \frac{Ra^2a_3A}{2}$; $b_5 = 2u_0\alpha^2Bm_1^2 + \frac{Ra^2a_3B}{2}$;

$b_6 = 2u_0\alpha^2Cm_3^2 + \frac{Ra^2a_3C}{2}$; $b_7 = 2u_0\alpha^2Dm_3^2 + \frac{Ra^2a_3D}{2}$;

$b_8 = 2u_0\alpha^2\alpha_c^2b_2 + \frac{Ra^2a_3b_2}{2}$; $b_9 = \frac{Ra^2Am_1}{2}$; $b_{10} = \frac{Ra^2Bm_1}{2}$;

$b_{11} = \frac{Ra^2Cm_3}{2}$; $b_{12} = \frac{Ra^2Dm_3}{2}$; $b_{13} = \frac{Ra^2b_2\alpha_c}{2}$; $b_{14} = Ra^2a_3p$;

$b_{15} = b_1 + \alpha^4 - a^2\alpha^2 - \frac{u_0Ra^2a_4}{t_0}$; $b_{16} = Ra^2a_3A$; $b_{17} = Ra^2a_3B$;

$b_{18} = Ra^2a_3C$; $b_{19} = Ra^2a_3D$; $b_{20} = Ra^2a_3b_2$; $c_1 = \frac{u_0ha_3A}{D_1}$;

$c_2 = \frac{u_0ha_3B}{D_1}$; $c_3 = \frac{u_0ha_3C}{D_1}$; $c_4 = \frac{u_0ha_3D}{D_1}$; $c_5 = \frac{u_0ha_3b_2}{D_1}$;

$c_6 = \frac{u_0ha_3b_1}{D_1} - \alpha^2 - \beta^2 + \frac{h^2a_4}{D_1t_0}$; $c_7 = \frac{u_0h\beta}{D_1Cosh[\beta]}$; $c_9 = \frac{u_0ha_3b_1}{D_1}\frac{h^2a_4}{d_1t_0}$;

⋆⋆⋆⋆⋆⋆⋆⋆⋆
ISSN(P):2319 − 3786
Malaya Journal of Matematik
ISSN(O):2321 − 5666
⋆⋆⋆⋆⋆⋆⋆⋆⋆